DALTON
FULL PAPER

Synthesis and electrochemistry of cobalt β-halogenated meso-tetraphenylporphyrins containing a nitrosyl axial ligand. Crystal structure of $(TPPBr_4NO_2)Co(NO)$

Karl M. Kadish,*[a] Zhongping Ou,[a] Xiaoyu Tan,[a] Tristano Boschi,[b] Donato Monti,[b] Vincenzo Fares*[c] and Pietro Tagliatesta*[b]

[a] *Department of Chemistry, University of Houston, Houston, TX 77204-5641, USA*
[b] *Dipartimento di Scienze e Tecnologie Chimiche, Universita' degli Studi di Roma, Tor Vergata, Via della Ricerca Scientifica-00133 Roma, Italy*
[c] *Istituto di Chimica dei Materiali, Area delle Ricerca di Roma, Montelibretti, via Salaria Km 29.300-C.P.10, 00016, Monterotondo, Roma, Italy*

Received 14th December 1998, Accepted 22nd March 1999

Three new cobalt porphyrins, two of which are coordinated by a nitrosyl group have been synthesized and characterized by spectral and electrochemical methods. The investigated compounds are represented as $(TPPBr_4)Co(NO)$, $(TPPBr_4NO_2)Co$ and $(TPPBr_4NO_2)Co(NO)$ where $TPPBr_4$ and $TPPBr_4NO_2$ are the dianions of 7,8,17,18-tetrabromo-5,10,15,20-tetraphenylporphyrin and 2-nitro-7,8,17,18-tetrabromo-5,10,15,20-tetraphenylporphyrin, respectively. Up to three oxidations and three reductions are observed for each compound in CH_2Cl_2 or pyridine containing 0.1 M TBAP. The first one-electron oxidation leads in all cases to formation of a Co(III) species while the first one-electron reduction leads invariably to a Co(I) porphyrin. The nitrosyl group remains coordinated to the Co(I) ion after electrogeneration of $[(TPPBr_4NO_2)Co(NO)]^-$ and $[(TPPBr_4NO_2)Co(NO)]^{2-}$ on the thin-layer spectroelectrochemical timescale and this enables the first UV–vis characterization of reduced cobalt porphyrins containing a bound NO axial ligand. The oxidation and reduction potentials of $(TPPBr_4)Co(NO)$, $(TPPBr_4NO_2)Co$ and $(TPPBr_4NO_2)Co(NO)$ are analyzed in terms of related redox reactions involving (TPP)Co(NO) and $(TPPBr_x)Co$ ($x = 0$–8) and $(TPPBr_4NO_2)Co(NO)\cdot 2CH_3CH_2OH$ was structurally characterized. The porphyrin ring possesses a saddle-shaped conformation as a result of a strong steric interaction which exists between the meso-phenyl and β-pyrrole groups on the macrocycle. The bound nitrosyl group has a bent conformation with a 125° angle and is disordered at two equivalent positions. The nitro substituted β-pyrrole group shows a tilted conformation and has a dihedral angle of 46° with respect to the mean plane of the porphyrin macrocycle in order to minimize interactions with the closest phenyl group.

Introduction

Synthetic iron and manganese tetraphenylporphyrins having halogen substituents on the β-pyrrole positions of the macrocycle are known to be good catalysts in the epoxidation of alkenes and the hydroxylation of alkanes.[1–10] The presence of electron-withdrawing substituents directly bound to the macrocycle makes this class of compounds highly efficient oxygen transfer catalysts because of their resistance to chemical degradation.[11–16] The redox potentials of β-halogenated porphyrins with Co or Fe central metal ions have been related to the degree of distortion of the macrocycle[17–19] and, as shown for $(TPPBr_x)FeCl$ where x varies from 0 to 8,[19a] there is a non-linear dependence of the first oxidation potential on the number of halogen substituents.

The electrochemical reactivity of iron and cobalt porphyrins with small molecules like CO[19] or NO[20] is also of importance with respect to understanding the reactions of naturally occuring hemoproteins like cytochromes and hemoglobins[21–23] but most studies have been limited in large part to simple tetraphenylporphyrin (TPP) or octaethylporphyrin (OEP) derivatives. We now present the synthesis and characterization of three new cobalt porphyrins, two of which are mono-nitrosyl derivatives. The investigated compounds are represented as $(TPPBr_4)Co(NO)$, $(TPPBr_4NO_2)Co(NO)$ and $(TPPBr_4NO_2)Co$, where $TPPBr_4$ and $TPPBr_4NO_2$ are the dianions of 7,8,17,18-tetrabromo-5,10,15,20-tetraphenylporphyrin and 2-nitro-7,8,17,18-tetrabromo-5,10,15,20-tetraphenylporphyrin respectively. All three porphyrins are investigated as to their electrochemistry in dichloromethane and pyridine and one of the derivatives, $(TPPBr_4NO_2)Co(NO)$, is structurally characterized.

Experimental

Chemicals

Benzonitrile (PhCN) was purchased from Aldrich Chemical Co. and distilled over P_2O_5 under vacuum prior to use. Absolute dichloromethane (CH_2Cl_2) stored over molecular sieves and pyridine (py) from Fluka Chemical Co. were used for electrochemistry without further purification. Dichloromethane (CH_2Cl_2), used in the synthesis of the compounds, was from Carlo Erba and distilled from P_2O_5 under argon prior to use. Tetra-*n*-butylammonium perchlorate (TBAP) was purchased from Sigma Chemical Co., recrystallized from ethyl alcohol and dried under vacuum at 40 °C for at least one week prior to use. Nitric oxide (99.5%) was obtained from Matheson and purified by passage through two consecutive traps containing KOH pellets and a cold trap (dry ice–acetone) to remove higher nitrogen oxides. $NOBF_4$ was purchased from Aldrich Chemical Co. and used as received. $(TPPBr_4)H_2$ and $(TPPBr_4)Co$ were synthesized as reported in the literature,[24] giving the antipodal tetrabromo derivatives.[17,25]

$(TPPBr_4)Co(NO)$. A 0.1 g sample of $(TPPBr_4)Co$ was dissolved in dry dichloromethane (30 mL) and 1.0 equivalent

$NOBF_4$ was added in small portions under argon as the color of the solution turned from reddish purple to dark greenish brown. A TLC plate analysis ($CHCl_3$–*n*-hexane; 7:3) showed the disappearance of the starting material and formation of a product with higher R_f. The solution was filtered and the solvent stripped off *in vacuo* to give a brown residue which was chromatographed on a silica gel column ($CHCl_3$–*n*-hexane; 7:3) and recrystallized from CH_2Cl_2/*n*-hexane. Yield 65%. IR in $CHCl_3$: ν_{NO}, 1692 cm^{-1}. UV–vis in $CHCl_3$, λ_{max}/nm: 439, 569. ^1H NMR ($CDCl_3$): δ 8.69 (4H, d, $J = 2$ Hz, β-pyrrole), 8.13–8.20 (8H, m, *o*-phenyl), 7.72–7.82 (12H, m, *p*-phenyl). FAB-MS: *m*/*z*, 987 $[M - NO]^+$. Calc. for $(TPPBr_4)Co(NO)\cdot 1/2CH_2Cl_2$: C, 50.40; H, 2.37; N, 6.34. Found: C, 50.56; H, 2.39; N, 6.60%.

The same $(TPPBr_4)Co(NO)$ product could be obtained by reaction of $(TPPBr_4)Co$ with NO gas in the solid state at room temperature. The final dark compound was recrystallized from $CHCl_3$–*n*-hexane (1:1). Yield 95%. The product obtained by this method is identical (TLC, UV–vis, NMR, FAB-MS) to that obtained from the stoichiometric reaction with $NOBF_4$. IR(Nujol): ν_{NO}, 1677 cm^{-1}. The apparent differences of the IR frequencies measured in solution and in the solid state is not unprecedented[26] and can be attributed to a solid state effect.

$(TPPBr_4NO_2)Co(NO)$. A 0.1 g sample of $(TPPBr_4)Co$ was allowed to react in CH_2Cl_2 with 3 equivalents of $NOBF_4$ under Ar for 5 hours. A TLC plate analysis ($CHCl_3$–*n*-hexane; 1:1) showed the disappearance of the starting material and formation of a product with lower R_f. The solution was filtered and the solvent evaporated under vacuum. The residue was chromatographed on a short silica gel column eluting with $CHCl_3$–*n*-hexane (1:1). Recrystallization from $CHCl_3$–*n*-hexane (1:1) gives dark-brown crystals of $(TPPBr_4NO_2)Co(NO)$. Yield 40%. IR in $CHCl_3$: ν_{NO}, 1710 cm^{-1}. UV–vis, in $CHCl_3$, λ_{max}/nm: 448, 569. ^1H NMR ($CDCl_3$): δ 8.84 (s, 1H, β-H pyrrole), 8.64 (d, $J = 5.0$ Hz, 1H, β-H pyrrole), 8.57 (d, $J = 5.0$ Hz, 1H, β-H pyrrole), 8.1–7.6 (m, 20H, phenyl). FAB-MS: *m*/*z* 1063 $[M + H]^+$; 1034 $[M + 2H - NO]^+$. Calc. for $(TPPBr_4NO_2)Co(NO)\cdot 1/2CH_2Cl_2$: C, 45.74; H, 2.05; N, 7.11%. Found: C, 45.72; H, 1.91; N, 6.87%. The same product could also be obtained from $(TPPBr_4)Co(NO)$ by reaction with $NOBF_4$ in CH_2Cl_2.

$(TPPBr_4NO_2)H_2$. $(TPPBr_4NO_2)Co(NO)$ (25 mg) was dissolved in a minimum amount of trifluoracetic acid (2.5 mL) and stirred under nitrogen as concentrated sulfuric acid (2.5 mL) was added to solution. The reaction mixture was allowed to stir under nitrogen overnight and then carefully poured into a flask containing 100 mL of crushed ice. The mixture was saturated with solid Na_2CO_3, diluted with water (100 mL) and extracted with $CHCl_3$ (3 × 50 mL).

The extract was washed with brine, dried over Na_2SO_4 and evaporated under reduced pressure to give crude $(TPPBr_4NO_2)H_2$ which was purified by column chromatography (SiO_2, CH_2Cl_2–*n*-hexane, 1:1) and recrystallized from $CHCl_3$–*n*-hexane, (1:2). Yield 90%. UV–vis in $CHCl_3$, λ_{max}/nm: 455, 553, 604, 709. ^1H NMR ($CDCl_3$): δ 8.7–8.6 (m, 3H, β-H pyrrole), 8.25–8.15 (m, 8 H, phenyl), 7.8–7.7 (m, 12H, phenyl), 2.1 (br s, 2H, NH pyrrole). FAB-MS: *m*/*z* 974 $[M - H]^+$. Calc. for $H_2(TPPBr_4NO_2)\cdot 2CH_2Cl_2$: C, 48.25; H, 2.55; N, 6.12. Found: C, 47.79; H, 2.10; N, 5.97%.

$(TPPBr_4NO_2)Co$. $(TPPBr_4NO_2)H_2$ (20 mg) was dissolved in 1,2-dichloroethane (75 mL) and a large excess of a $Co(OAc)_2$ saturated methanol solution was added (5 mL). The reaction mixture was refluxed overnight under nitrogen and then washed with brine (3 × 100 mL), dried over Na_2SO_4 and evaporated under reduced pressure after which the residue was chromatographed on a silica gel column (CH_2Cl_2–*n*-hexane, 3:2). The first greenish-brown band was collected, evaporated and recrystallized (CH_2Cl_2–*n*-hexane, 1:1) to give the title compound. Yield 90%. UV–vis in $CHCl_3$, λ_{max}/nm: 448, 559. FAB-MS: *m*/*z*, 1031 $[M - H]^+$. Calc. for $(TPPBr_4NO_2)Co\cdot CH_2Cl_2$: C, 48.38; H, 2.26; N, 6.27. Found: C, 48.49; H, 2.69; N, 5.93%.

Instrumentation

Cyclic voltammetry was carried out with an EG&G Model 173 potentiostat or an IBM Model EC 225 Voltammetric Analyzer. Current–voltage curves were recorded on an EG&G Princeton Applied Research Model Re-0151 X-Y recorder. A three electrode system was used and consisted of a glassy carbon or platinum button working electrode, a platinum wire counter electrode and a saturated calomel reference electrode (SCE). This reference electrode was separated from the bulk of the solution by a fritted-glass bridge filled with the solvent–supporting electrolyte mixture. All potentials are referenced to the SCE.

UV–vis spectroelectrochemical experiments were performed with a home-built platinum thin-layer cell of the type described in the literature.[27] Potentials were applied and monitored with an EG&G Princeton Applied Research model 173 potentiostat. UV–vis spectra of the neutral, oxidized and reduced complexes were recorded with an HP 8453 UV-visible spectrophotometer.

NMR spectra were recorded on a Bruker AM-300 spectrometer as $CDCl_3$ solutions with $SiMe_4$ as internal standard. IR spectra of the neutral complexes were recorded on a Perkin-Elmer 982 spectrophotometer while spectral changes during oxidation or reduction of the porphyrins were monitored on a FTIR Nicolet 550 Magna-IR spectrometer using a specially constructed light-transparent three-electrode cell.[28] Mass spectra were recorded on a VG-quattro mass spectrometer using 3-nitrobenzyl alcohol (NBA) as a matrix. Elemental analyses were carried out by the Analytical Laboratory of the University of Padova.

Structural determination of $(TPPBr_4NO_2)Co(NO)\cdot 2CH_3CH_2OH$

Crystals of $(TPPBr_4NO_2)Co(NO)$ were grown by slow diffusion of *n*-hexane into a chloroform–ethanol solution (99:1) containing the title compound. The compound crystallizes as dark red irregular platelets, unstable in air, and a selected crystal was therefore fixed inside a Lindemann capillary in the presence of the mother liquor. Data were collected on a Huber/Ital Structure automated diffractometer equipped with a molybdenum source and a graphite monochromator and corrected for absorption (ψ-scan method), Lorentz and polarization effects. The structure was solved by direct methods by using the SIR92 program,[29] and refined by full-matrix least-squares methods.

CCDC reference number 186/1398.

Results and discussion

Synthesis

The reaction of four-coordinate $(TPPBr_4)Co$ in CH_2Cl_2 with stoichiometric amounts of $NOBF_4$ or with an excess of NO gas results in the formation of the same mono-nitrosyl derivative, $(TPPBr_4)Co(NO)$, in 65–95% isolated yield. However, when an excess of $NOBF_4$ was used for the purpose of obtaining a bis(nitrosyl) derivative, a different product was isolated in good yield.

A crystal structure of the isolated compound (see following pages) shows the presence of a nitro-group bound directly at the β-position of the $TPPBr_4$ macrocycle and only one NO group bound at the metal center to give $(TPPBr_4NO_2)Co(NO)$. This compound, in our opinion, derives from an electrophilic attack of NO^+ on $(TPPBr_4)Co(NO)$ to give a transient $(TPPBr_4NO)Co(NO)$ species followed by oxidation to give the final $(TPPBr_4NO_2)Co(NO)$ product. In order to prove the validity of this

hypothesis, $(TPPBr_4)Co(NO)$ was subjected to a reaction with $NOBF_4$ which leads *via* a fast conversion to the same $(TPPBr_4NO_2)Co(NO)$ derivative. An oxidation reaction is therefore necessary to convert the proposed β-nitrosyl intermediate, $(TPPBr_4NO)Co(NO)$, to the final product.

A similar type of oxidation has been reported for the conversion of aromatic compounds to nitro derivatives.[30] The reaction of NO^+ with Co(II) porphyrins is known to give a Co(II) mono-nitrosyl porphyrin π-cation radical and this species can be chemically reduced by using cobaltocene to give the neutral Co(II) nitrosyl porphyrin.[31] The formation of $(TPPBr_4NO_2)Co(NO)$ from $(TPPBr_4)Co$ requires no chemical reducing agent and the solvent is most likely involved in the one-electron reduction.

The introduction of a single nitro group at the β-position of a tetraphenylporphyrin macrocyle followed by transformation of the nitro group into an –OR or –R group has been reported in the literature,[32,33] but no information is available regarding the introduction of nitro groups onto the skeleton of β-halogenated porphyrins. Furthermore, a deactivation of $(TPPBr_4)Co$ towards direct electrophilic attack by NO_2^+ occurs due to the four strongly electron withdrawing groups on the macrocycle and a nitration reaction gives only the 4-nitrophenyl derivative.[34]

The introduction of the NO_2 moiety in the pyrrolic β-position is clearly evidenced by the ^1H NMR spectral features of $(TPPBr_4NO_2)Co(NO)$ compared to that of the parent $(TPPBr_4)Co(NO)$ porphyrin derivative. The β-H pyrrolic doublet is turned into a more complex set of signals. This can be ascribed to the lowering of the degree of symmetry of the resulting macrocycle. A deshielding effect exerted by the NO_2 group on the vicinal proton is also observed (see Experimental section).

A summary of the proposed reaction sequences to give the two isolated nitrosyl derivatives, $(TPPBr_4)Co(NO)$ and $(TPPBr_4NO_2)Co(NO)$, is shown in Scheme 1.

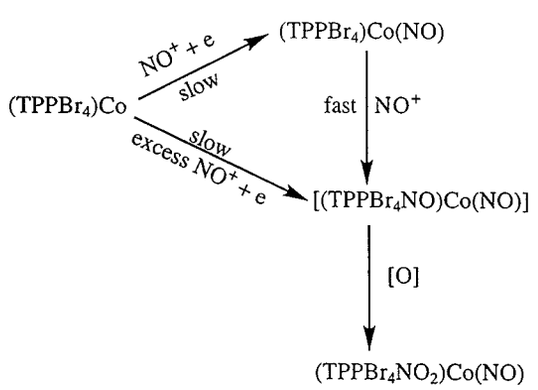

Scheme 1

Crystal structure of $(TPPBr_4NO_2)Co(NO)\cdot 2CH_3CH_2OH$

Crystal data and details of data collection and structure refinement are given in Table 1. Refinement was anisotropic for non-H atoms, except for the phenyl rings (refined as rigid groups), the nitrosyl oxygen, disordered at two positions, and the CH_3CH_2OH solvent molecules, which are affected by a severe disorder. It was not possible to rationalize the two groups of peaks found around two centers of symmetry (0, 0, 0 and 0, 0, 1/2 respectively). The best fit was obtained by considering six and five "partial" atoms with refined site occupation factors in the range 0.25–1.00.

The molecular structure of $(TPPBr_4NO_2)Co(NO)$ is shown in Figs. 1 and 2 and selected bond lengths and angles are reported in Table 2. The low quality of the available crystals limits the accuracy of the geometrical parameters, affected by the rather high standard deviations. The cobalt is in a square

Table 1 Crystal data and structure refinement for $(TPPBr_4NO_2)Co(NO)\cdot 2CH_3CH_2OH$

Empirical formula	$C_{48}H_{35}N_6O_5Br_4Co$
M	1154.4
T/K	293(3)
λ/Å	0.71069
Crystal structure	Triclinic
Space group	$P\bar{1}$
a/Å	13.253(6)
b/Å	13.595(7)
c/Å	14.537(6)
α/°	102.51(4)
β/°	111.73(4)
γ/°	106.35(5)
V/Å^3	2177(2)
Z	2
D_c/g cm^{-3}	1.761
μ/mm^{-1}	4.122
$F(000)$	1144
Crystal size/mm	0.4 × 0.4 × 0.1
θ range for data collection/°	1.5–27.5
Index ranges	$-2 \leqslant h \leqslant 13$, $-15 \leqslant k \leqslant 13$, $-16 \leqslant l \leqslant 15$
No. reflections collected	2721
No. independent reflections	2399 [R(int) = 0.01]
Refinement method	Full-matrix least-squares
Data/restraints/params	2342/48/398
Goodness-of-fit on F^2	0.9
Final R indices ($I > 2\sigma(I)$)	$R1$ = 0.0587, $wR2$ = 0.0823
R indices (all data)	$R1$ = 0.0642, $wR2$ = 0.1108
Largest diff. peak, hole/e Å^{-3}	0.78, −0.63

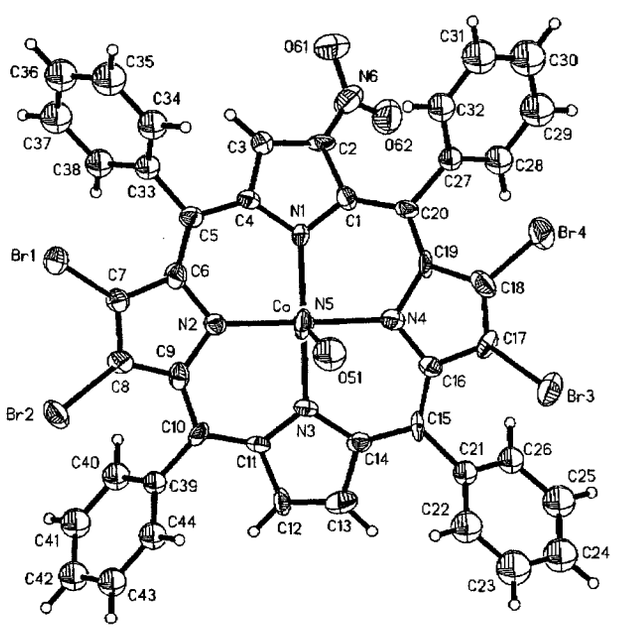

Fig. 1 ORTEP[53] drawing of $(TPPBr_4NO_2)Co(NO)$ showing the atom-numbering scheme. Ellipsoids are at the 30% probability level.

pyramidal CoN_5 environment; it is displaced by 0.21 Å above the basal plane towards the axially coordinated nitrosyl group which is bent as expected for a five-coordinate nitrosyl–cobalt complex.[35] The nitrosyl oxygen atom is disordered at two, O(51) and O(52), crystallographically independent positions, the angle O(51)–N(5)–O(52) being 56°, and the dihedral angles that the Co–N(5)–O(51) and Co–N(5)–O(52) planes form with the Co–N(3) vector are 41 and 29°, respectively. Owing to the disorder and a libration effect, the N–O distance is shorter (av. 1.081 Å) than the value of 1.195 Å reported for [T(*p*-OCH_3)PP]Co(NO) [where T(*p*-OCH_3)PP represents 5,10,15,20-tetra-(4-methoxyphenyl)porphyrin].[31]

The Co–N–O angle of 125° (av.) and the Co–N_{ax} distance of 1.827 Å are comparable with values found in analogous nitrosyl cobalt porphyrin complexes.[31,36] Similar structural features can

Table 2 Selected bond distances (Å) and angles (°), with e.s.d.s in parentheses

Co–N(1)	1.933(9)	Co–N(2)	1.971(13)
Co–N(3)	1.911(9)	Co–N(4)	1.966(14)
Co–N(5)	1.827(21)	N(5)–O(51)	1.054(34)
N(5)–O(52)	1.108(48)	C(2)–N(6)	1.411(25)
C(7)–Br(1)	1.836(13)	C(8)–Br(2)	1.866(18)
C(17)–Br(3)	1.849(14)	C(18)–Br(4)	1.888(21)
Averaged:			
N–C_α	1.39(2)	C_α–C_β	1.45(2)
C_α–$C_{methine}$	1.38(2)	C_β–C_β	1.34(2)
$C_{methine}$–C_{phenyl}	1.47(2)		
N(1)–Co–N(2)	89.1(5)	N(1)–Co–N(3)	161.7(6)
N(2)–Co–N(3)	90.1(5)	N(1)–Co–N(4)	90.0(5)
N(2)–Co–N(4)	177.4(6)	N(3)–Co–N(4)	90.0(5)
N(1)–Co–N(5)	98.1(6)	N(2)–Co–N(5)	89.7(7)
N(3)–Co–N(5)	100.2(6)	N(4)–Co–N(5)	92.8(7)
Co–N(5)–O(51)	123.8(19)	Co–N(5)–O(52)	125.6(25)
O(61)–N(6)–O(62)	121.5(19)		

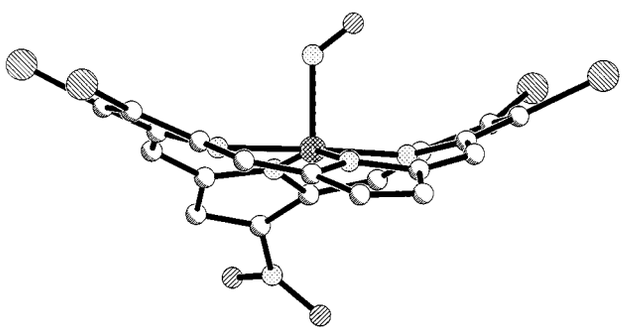

Fig. 2 Side view of $(TPPBr_4NO_2)Co(NO)$. Only one position of the disordered nitrosyl oxygen is shown. Phenyl rings have been omitted for clarity.

be observed in the related five-coordinated nitrosyl–iron porphyrins.[26,37]

Given the presence of nine bulky peripheral substituents (four phenyl rings at the meso-carbons C_m, four bromine atoms at the β-carbons C_β of two opposite pyrroles and a nitro-group at another β-carbon), the macrocycle is strongly distorted towards a saddle-shaped conformation ("sad" symmetry or B_{1u} non-planar distortion)[38,39] similar to that of $[(TPPBr_4)Fe]_2O$,[40] where the five-coordinated iron is complexed by a tetrabromo-substituted tetraphenylporphyrin. The pyrrole rings are tilted alternately above and below the mean porphyrin plane, with the β-carbons displaced by 0.78–1.03 Å. Superimposed onto the main "sad" distortion, a secondary "ruf" (or B_{2u}) distortion can be noted, as evidenced by the displacement values of the C_m atoms (0.08–0.23 Å) and the slight twist of the opposite pyrrole rings with respect to each other by *ca.* 17°. The dihedral angles between the phenyl rings and the porphyrin macrocycle are in the range of 43–55° (av. 49°), close to values found in $[(TPPBr_4)Fe]_2O$, (49–62°, av. 56°)[40] and other highly distorted saddle-shaped halogenated porphyrins (mean values between 44 and 59°).[41–43]

Table 3, in which the main geometrical features of analogous cobalt porphyrin complexes are listed, shows the strong dependence of the phenyl dihedral angles on the type and degree of distortion. In the present case, the twisting values are due to a subtle balance of the weak H–H repulsive (2.72–3.20 Å) and H–Br attractive (3.43–3.69 Å) interactions between the phenyl hydrogens and H(C_β) or Br(C_β), respectively.

The same dependence can be noted for the Co–N_{por} distances reported in Table 3; within the series of CoN_4 porphyrin complexes, they range from 1.97 Å for planar compounds to 1.95 Å for "ruf" and 1.93–1.94 Å for "sad" distorted compounds.[44–48] For the three known symmetrically substituted square-pyramidal CoN_5 porphyrin complexes, the reported Co–N_{por} distances are 1.978 Å for planar conformations,[36,48] while two different values (1.967 and 1.978 Å, respectively) were found for the "ruf" distorted one.[31] The title compound contains different electron-acceptor peripheral substituents which are asymmetrically positioned. It is noteworthy to point out the strong σ-influence of such groups on the Co–N_{por} bonds which lengthen on passing from the unsubstituted pyrrole [Co–N(3) 1.911 Å] to the mono-nitro substituted one [Co–N(1) 1.933 Å] and then to the bis(bromo) complex which is substituted at two pyrrole rings [Co–N(2) 1.971 Å, Co-N(4) 1.966 Å].

Finally, the nitro-group makes a dihedral angle of 46° with the mean plane of the porphyrin core and is almost parallel to the closest phenyl ring in order to maximize the distance between the overcrowded neighboring atoms.

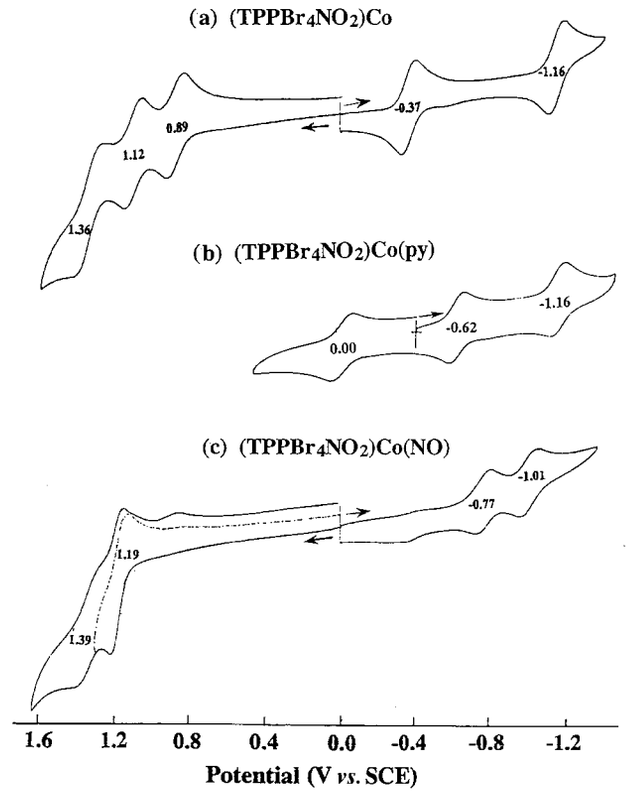

Fig. 3 Cyclic voltammograms of (a) $(TPPBr_4NO_2)Co$ and (c) $(TPPBr_4NO_2)Co(NO)$ in CH_2Cl_2 and (b) $(TPPBr_4NO_2)Co(py)$ in pyridine containing 0.1 M TBAP.

Electrochemistry of $(TPPBr_4NO_2)Co$ and $(TPPBr_4NO_2)Co(NO)$

Fig. 3 illustrates cyclic voltammograms of $(TPPBr_4NO_2)Co$ and $(TPPBr_4NO_2)Co(NO)$ in CH_2Cl_2 and $(TPPBr_4NO_2)Co$ in pyridine containing 0.1 M TBAP. Under the latter solution conditions, the Co(II) complex exists as a mono-pyridine adduct. Each compound undergoes two reductions and one to three oxidations depending upon the solvent and specific axial ligand. The Co(II)/(I) reduction of $(TPPBr_4NO_2)Co$ is located at −0.37 V in CH_2Cl_2 and this potential can be compared to $E_{1/2}$ values of −0.62 and −0.77 for reduction of $(TPPBr_4NO_2)Co(py)$ in pyridine and $(TPPBr_4NO_2)Co(NO)$ in CH_2Cl_2, respectively. The negative shift of 250–400 mV in reduction potentials upon axial ligand coordination is consistent with results in the literature for other cobalt porphyrins under the same experimental conditions[49,50] and can be explained by the fact that the pyridine and NO ligands bind more strongly to the Co(II) porphyrin than to the reduced Co(I) form of the complex. The data in Fig. 3 are also consistent with results in the literature indicating a very strong ligand binding of Co(III) porphyrins by pyridine[50] and a moderately strong stabilization

Table 3 Summary of the main geometrical features in several cobalt(II) porphyrin complexes

Complex	Chromophore	Displacements[a]/Å C_m	Displacements[a]/Å C_α	Conformation	Ph-dihedral angles[b]/°	Co–N_{por}/Å	Co–N_{ax}/Å	Ref.
$(TF_5PP)Co$	CoN_4			planar	>70	1.976		44
$[T(p\text{-}Me_2N)F_4PP]Co$	CoN_4			planar	>70	1.971		44
(TPP)Co	CoN_4	42	17	ruf	80.2	1.942		45
(TFPrP)Co	CoN_4			sad	—	1.937		46
(OETPP)Co	CoN_4			sad	46.1	1.929		47
(TPP)Co(MIm)	CoN_5	6	5	planar	72.9	1.977	2.157	48
(TPP)Co(NO)	CoN_5			planar	>70	1.978	1.833	36
$[T(p\text{-}OCH_3)PP]Co(NO)$	CoN_5	31	18	ruf	>65	1.967 1.978	1.856	31
$(TPPBr_4NO_2)Co(NO)$	CoN_5	17	89	sad	49.1	1.911 1.933 1.966 1.971	1.827	Tw[c]

Abbreviations: TF_5PP = 5,10,15,20 = tetrakis(2,3,4,5,6-pentafluorophenyl)porphyrinate; $[T(p\text{-}Me_2N)F_4PP]$ = 5,10,15,20-tetrakis(4-*N*,*N*-dimethylamino-2,3,5,6-tetrafluorophenyl)porphyrinate; TFPrP = 5,10,15,20-tetrakis(heptafluoropropyl)porphyrinate; OETPP = 2,3,7,8,12,13,17,18-octaethyl-5,10,15,20-tetraphenylporphyrinate; MIm = 1-methylimidazole. [a] Averaged absolute values in units 0.01 Å. [b] Averaged values. [c] Tw = this work.

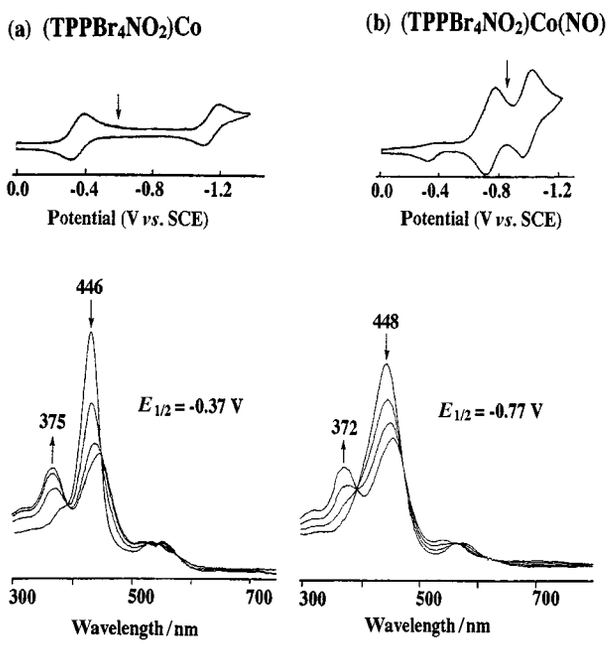

Fig. 4 Thin-layer cyclic voltammograms and thin-layer spectral changes during the first controlled-potential reduction of (a) $(TPPBr_4NO_2)Co$ and (b) $(TPPBr_4NO_2)Co(NO)$ in CH_2Cl_2, 0.2 M TBAP.

of the Co(II) porphyrins by NO.[31,49,51] This results in a 300 mV *positive* shift in the Co(II)/Co(III) oxidation potential upon going from $(TPPBr_4NO_2)Co$ ($E_{1/2}$ = 0.89 V) to $(TPPBr_4NO_2)$-Co(NO) ($E_{1/2}$ = 1.19) and an 890 mV *negative* shift in oxidation potential upon going from $(TPPBr_4NO_2)Co$ to $(TPPBr_4NO_2)$-Co(py) ($E_{1/2}$ = 0.00 V).

The second reduction of $(TPPBr_4NO_2)Co$ occurs at the same potential in CH_2Cl_2 and pyridine and the $E_{1/2}$ value of −1.16 V can be compared to a reversible half-wave potential of −1.01 V for the second one-electron reduction of $(TPPBr_4NO_2)Co(NO)$ in CH_2Cl_2. The first result is consistent with the known lack of pyridine binding to Co(I) porphyrins[49,50] and the second with the coordination of the NO ligand to singly and doubly reduced $(TPPBr_4NO_2)Co(NO)$ on the timescale of the voltammetric measurement. Similar results are seen for reactions involving complexes of (TPP)Co[49,50] and substituted (TPP)Co.[31]

Thin-layer cyclic voltammograms and the related thin-layer UV-vis spectra obtained during controlled-potential electroreduction of $(TPPBr_4NO_2)Co$ and $(TPPBr_4NO_2)Co(NO)$ in CH_2Cl_2 containing 0.2 M TBAP are shown in Fig. 4. The final Co(I) spectra are similar in shape to those obtained after the metal-centered reduction of $(TPPBr_x)Co^{II}$ where x = 6, 7 or 8.[52] The first reduction of $(TPPBr_4NO_2)Co^{II}$ occurs at the same potential as the Co^{II}/Co^{I} reaction of $(TPPBr_8)Co^{II}$ (−0.35 V in PhCN),[52] thus suggesting a similar effect of the two macrocycles on this redox reaction.

The electrochemical reduction of (TPP)Co(NO)[51] and related $[T(p\text{-}X)PP]Co(NO)$[31] complexes (X = OMe, Me, CF_3 or CN) is followed by a rapid loss of the NO axial ligand on the timescale of spectroelectrochemistry and the actual site of electron transfer could not previously be unambiguously ascertained since the only characterized porphyrin products in solution were invariably the uncoordinated Co(I) species.[51] This is not the case for $(TPPBr_4NO_2)Co(NO)$ which is reversibly reduced to give $[(TPPBr_4NO_2)Co(NO)]^-$ and $[(TPPBr_4NO_2)$-$Co(NO)]^{2-}$ on the thin-layer voltammetric timescale.

The singly reduced species was characterized by UV-vis spectroelectrochemistry prior to a slow loss of the NO axial ligand and examples of the spectroelectrochemical data are shown in Fig. 4 which illustrates results obtained during the first one-electron reduction of $(TPPBr_4NO_2)Co$ and $(TPPBr_4NO_2)$-$Co(NO)$ in CH_2Cl_2. These spectral changes are reversible and similar to each other, thus indicating that $[(TPPBr_4NO_2)$-$Co^{I}(NO)]^-$ is formed under the given experimental conditions. A slow NO loss occurs after reduction (as indicated by the anodic peak at E_{pa} = −0.33 V in Fig. 4b). However, as seen in the figure, a good reversibility of the voltammogram is obtained on the thin-layer timescale.

Electrooxidation

$(TPPBr_4NO_2)Co$ undergoes three reversible one-electron oxidations (at $E_{1/2}$ = 0.89, 1.12 and 1.36 V), the first of which leads to a Co(III) porphyrin while the second and third generate a Co(III) porphyrin π cation radical and dication. $(TPPBr_4NO_2)$-$Co(NO)$ is also converted to a Co(III) dication in CH_2Cl_2, but this reaction occurs in two steps, the first of which involves two overlapping one-electron transfer steps at $E_{1/2}$ = 1.19 V.

Two well resolved processes are seen upon oxidation of (TPP)Co(NO) ($E_{1/2}$ = 1.01 and 1.25 V)[51] and the voltammetric data for $(TPPBr_4NO_2)Co(NO)$ can then be interpreted in terms of decreased NO binding by the singly and/or doubly oxidized species and a rapid loss of this axial ligand after the two electron oxidation. Neutral $(TPPBr_4NO_2)Co(NO)$ shows a strong NO stretching band at 1706 cm^{-1} in CH_2Cl_2, 0.2 M TBAP, but an NO band of the coordinated ligand could not be detected after the first oxidation. The UV–vis spectrum of the final porphyrin product after the two-electron oxidation of $(TPPBr_4NO_2)Co(NO)$ (Fig. 5b) is almost identical to that of $(TPPBr_4NO_2)Co$ after the stepwise abstraction of two electrons

Table 4 Half-wave potentials (V *vs.* SCE) for reduction and oxidation of cobalt porphyrins in CH_2Cl_2 or pyridine, 0.1 M TBAP

		Oxidation			Reduction	
Solvent	Compound	3rd	2nd	1st	1st	2nd
CH_2Cl_2	(TPP)Co[a]	1.16	0.97	0.78	−0.85	−2.05
	($TPPBr_4$)Co	1.21	1.02	0.81	−0.56	−1.61[c]
	($TPPBr_4NO_2$)Co	1.36	1.12	0.89	−0.37	−1.16
CH_2Cl_2	(TPP)Co(NO)[a]		1.25	1.01	−1.18	−1.75
	($TPPBr_4$)Co(NO)		1.26	1.06	−1.10	−1.60[c]
	($TPPBr_4NO_2$)Co(NO)	1.39	1.19[d]	1.19[d]	−0.77	−1.01
py	(TPP)Co(py)[b]			−0.21	−1.03	
	($TPPBr_4$)Co(py)			−0.14	−0.81	−1.57[c]
	($TPPBr_4NO_2$)Co(py)			0.00	−0.62	−1.16

[a] Ref. 51. [b] Ref. 50(*a*). [c] E_{pc}, at scan rate 100 mV s^{-1}. [d] Two overlapping one-electron processes.

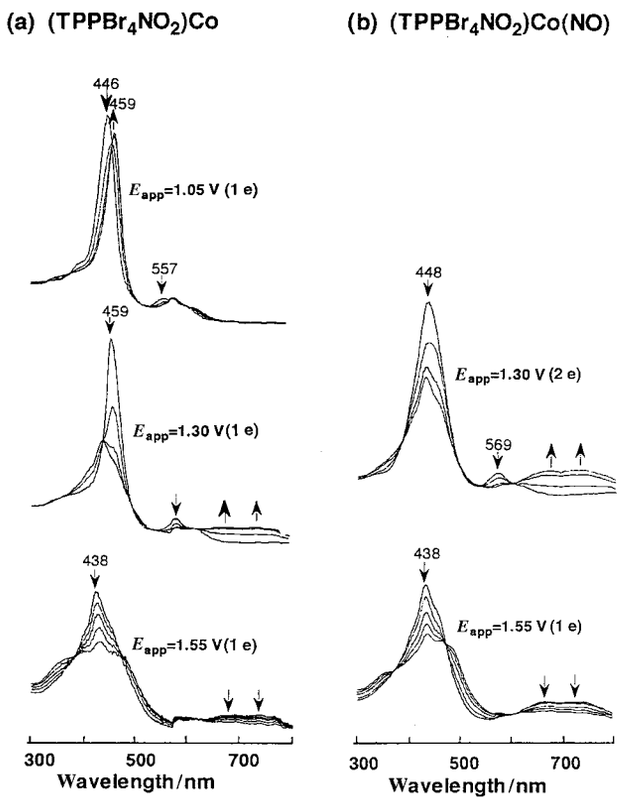

Fig. 5 Thin-layer spectral changes during controlled potential oxidations of (a) ($TPPBr_4NO_2$)Co and (b) ($TPPBr_4NO_2$)Co(NO) in CH_2Cl_2, 0.2 M TBAP.

(Fig. 5a). The third one-electron oxidation of the two compounds also occurs at similar potentials of 1.36 and 1.39 V (see Fig. 3). These results are both consistent with the loss of NO after oxidation and the redox processes shown below for ($TPPBr_4NO_2$)Co(NO).

$$(TPPBr_4NO_2)Co(NO) \overset{1.19\ V}{\rightleftharpoons} [(TPPBr_4NO_2)Co(NO)]^{2+} + 2e$$

$$\xrightarrow[-NO]{Fast} [(TPPBr_4NO_2)Co]^{2+}$$

$$[(TPPBr_4NO_2)Co]^{2+} \overset{1.39\ V}{\rightleftharpoons} [(TPPBr_4NO_2)Co]^{3+} + e$$

Effect of electron-withdrawing substituents on redox reactions

A summary of redox potentials for the investigated compounds and related derivatives of (TPP)Co and ($TPPBr_4$)Co is given in Table 4. The addition of electron-withdrawing Br and NO_2 substituents to the TPP macrocycle shifts the redox potentials in a positive direction with respect to the unsubstituted complex, with the largest magnitude of the shift being for reductions and the smallest for oxidations. As seen in Table 4, the absolute potential difference between the second reduction of (TPP)Co ($E_{1/2} = -2.05$ V) and the second reduction of ($TPPBr_4NO_2$)Co ($E_{1/2} = -1.16$ V) amounts to 0.89 V in CH_2Cl_2 as compared to differences of 0.48 and 0.11 V between the first reduction and first oxidation of the same two compounds, respectively. Similar results are observed for the (por)Co(py) and (por)Co(NO) derivatives although in these cases, as discussed in the above section, the nature of the coordinated axial ligand (py or NO) will also influence to a large extent the potentials for oxidation and reduction.

Larger differences in redox potential are seen upon going from $TPPBr_4$ to $TPPBr_4NO_2$ than between TPP and $TPPBr_4$ as a macrocycle. This can be associated with the large electron-withdrawing ability of the NO_2 group as well as with a change in planarity of the macrocycle upon going from (TPP)Co or ($TPPBr_4$)Co to ($TPPBr_4NO_2$)Co which shows a large distortion in the macrocycle as indicated in Fig. 1. Other trends are also seen from the data, the most notable of which are the potential differences between the first and second reductions which systematically shift from 1.20 V in the case of (TPP)Co, to 0.79 V in the case of ($TPPBr_4NO_2$)Co. A decrease in separation between the first reduction and first oxidation of the two compounds is also observed ($\Delta E_{1/2}$ shifts of 1.63 and 1.26 V respectively) but at the same time, the absolute potential difference between the first and second oxidations shift in the opposite direction by a small amount, going from 0.19 V in the case of (TPP)Co to 0.23 V in the case of ($TPPBr_4NO_2$)Co. Finally, it should be pointed out that the HOMO–LUMO gap of the (por)Co derivatives also decreases as the solvent changes from CH_2Cl_2 to pyridine. For example, the $\Delta E_{1/2}$(ox − red) is 1.26 V for ($TPPBr_4NO_2$)Co in CH_2Cl_2, but only 0.62 V in pyridine.

In summary, the binding of NO is stronger to the reduced forms of ($TPPBr_4NO_2$)Co and weaker to its oxidized forms as compared to the same chemical reactivity involving (TPP)Co or ($TPPBr_4$)Co. This difference in stability may be related to the much easier reduction and slightly harder oxidation which results from the electron-withdrawing substituents on ($TPPBr_4NO_2$)Co(NO) or it may be related to the non-planarity of the ($TPPBr_4NO_2$)Co(NO) macrocycle as compared to (TPP)Co and ($TPPBr_4$)Co. Studies of other cobalt porphyrins with different substitution patterns are now underway in order to clarify this point.

Acknowledgements

The support of the Robert A. Welch Foundation (Grant E-680, K. M. K.) and the CNR (P. T.) are gratefully acknowledged.

References

1 T. C. Bruice, *Acc. Chem. Res.*, 1991, **24**, 243.
2 I. Tabushi, *Coord. Chem. Rev.*, 1988, **86**, 1.
3 D. Mansuy, *Pure Appl. Chem.*, 1987, **59**, 759.
4 B. Meunier, *Chem. Rev.*, 1992, **92**, 1411.

5 D. Mansuy, *The Activation of Dioxygen and Homogeneous Catalytic Oxidation*, Plenum Press, New York and London, 1993, pp. 347–358.
6 T. C. Bruice, *Mechanistic Principles of Enzyme Activity*, eds. J. F. Liberman and A. Greenberg, VCH Publishers, New York, 1988, ch. 8.
7 T. J. McMurry and J. T. Groves, in *Cytochrome P-450: Structure, Mechanism and Biochemistry*, ed. P. R. Ortiz de Montellano, Plenum Press, New York, 1986, ch. 1.
8 T. G. Traylor, Y. S. Byun, P. S. Traylor, P. Battioni and D. Mansuy, *J. Am. Chem. Soc.*, 1991, **113**, 7821.
9 T. G. Traylor, *Acc. Chem. Res.*, 1981, **14**, 102.
10 P. S. Traylor, D. Dolphin and T. G. Traylor, *J. Chem. Soc.*, *Chem. Commun.*, 1984, 279.
11 A. M. Gonsalves, R. A. W. Johnstone, M. M. Pereira, J. Shaw and J. F. Sobral, *Tetrahedron Lett.*, 1991, **32**, 1355.
12 T. G. Traylor and S. Tsuchiya, *Inorg. Chem.*, 1987, **26**, 1338.
13 M. W. Grinstaff, M. G. Hill, J. A. Labinger and H. B. Gray, *Science*, 1994, **264**, 1311.
14 P. E. Ellis and J. E. Lyons, *J. Chem. Soc. Chem. Commun.*, 1989, 1315.
15 P. E. Ellis and J. E. Lyons, *Coord. Chem. Rev.*, 1990, **105**, 181.
16 J. E. Lyons and P. E. Ellis, *Metalloporphyrins in Catalytic Oxidation*, ed. R. Sheldon, Marcel Dekker, New York, 1994, pp. 297–324.
17 P. Ochsenbein, K. Ayougou, D. Mandon, J. Fisher, R. Weiss, R. N. Austin, K. Jayaraj, A. Gold, J. Terner and J. Fajer, *Angew. Chem.*, *Int. Ed. Engl.*, 1994, **33**, 348.
18 K. M. Kadish, F. D'Souza, A. Villard, M. Autret, E. Van Caemelbecke, P. Bianco, A. Antonini and P. Tagliatesta, *Inorg. Chem.*, 1994, **33**, 5169.
19 (*a*) P. Tagliatesta, J. Li, M. Autret, E. Van Caemelbecke, A. Villard, F. D'Souza and K. M. Kadish, *Inorg. Chem.*, 1996, **35**, 5570; (*b*) X. H. Mu and K. M. Kadish, *Inorg. Chem.*, 1989, **28**, 3743; (*c*) Y. Hu, B. C. Han, L. Y. Bao, X. H. Mu and K. M. Kadish, *Inorg. Chem.*, 1991, **30**, 2444; (*d*) K. M. Kadish, J. Li, E. Van Caemelbecke, Z. Ou, N. Guo, M. Autret, F. D'Souza and P. Tagliatesta, *Inorg. Chem.*, 1997, **36**, 6292.
20 (*a*) M. Autret, S. Will, E. Van Caemelbecke, J. Lex, M. Gisselbrecht, E. Gross, E. Vogel and K. M. Kadish, *J. Am. Chem. Soc.*, 1994, **116**, 9141; (*b*) X. H. Mu and K. M. Kadish, *Inorg. Chem.*, 1988, **27**, 4720.
21 J. R. Stone and M. A. Marletta, *Biochemistry*, 1994, **33**, 5636 and refs. therein.
22 A. E. Yu, S. Hu, T. G. Spiro and J. N. Burstyn, *J. Am. Chem. Soc.*, 1994, **116**, 4117.
23 E. Antonini and M. Brunori, *Hemoglobin and Myoglobin in their Reactions with Ligands*, Elsevier, New York, 1971.
24 (*a*) H. J. Callot, *Bull. Soc. Chim. Fr.*, 1974, **7**–**8**, 1492; (*b*) J.-H. Fuhrhop and K. M. Smith, *Porphyrins and Metalloporphyrins*, ed. K. M. Smith, Elsevier, New York, 1975, ch. 19.
25 M. J. Crossley, P. L. Burn, S. S. Chew, F. B. Cuttance and I. A. Newsom, *J. Chem. Soc.*, *Chem. Commun.*, 1991, 1564.
26 M. K. Ellison and W. R. Scheidt, *J. Am. Chem. Soc.*, 1997, **119**, 7404.
27 X. Q. Lin and K. M. Kadish, *Anal. Chem.*, 1985, **57**, 1498.
28 K. M. Kadish, X. H. Mu and X. Q. Lin, *Electroanalysis*, 1989, **1**, 35.
29 A. Altomare, G. Cascarano, C. Giacovazzo, A. Guagliardi, M. C. Burla, C. Polidori and M. Camalli, *Appl. Crystallogr.*, 1994, **27**, 435.
30 (*a*) S. Uemura and A. Toshimitsu, *J. Chem. Soc.*, *Perkin Trans. 1*, 1978, 1076; (*b*) E. C. Taylor, R. Danforth and A. McKillop, *J. Org. Chem.*, 1973, **38**, 2088.
31 (*a*) G. B. Richter-Addo, S. J. Hodge, G. Yi, A. Khan, T. Ma, E. Van Caemelbecke, N. Guo and K. M. Kadish, *Inorg. Chem.*, 1996, **35**, 6530; (*b*) G. B. Richter-Addo, S. J. Hodge, G. Yi, A. Khan, T. Ma, E. Van Caemelbecke, N. Guo and K. M. Kadish, *Inorg. Chem.*, 1997, **36**, 2696.
32 H. K. Hombrecher, V. M. Gherdan, S. Ohm, J. A. S. Cavaleiro, M. G. P. M. S. Neves and M. F. Condesso, *Tetrahedron*, 1993, **49**, 8569.
33 A. Giraudeau, H. J. Callot, J. Jordan, I. Ezhar and M. Gross, *J. Am. Chem. Soc.*, 1979, **101**, 3857.
34 P. Tagliatesta, D. Monti and T. Boschi, unpublished work.
35 (*a*) B. B. Wayland, J. V. Minkiewicz and M. E. Abd-Elmageed, *J. Am. Chem. Soc.*, 1974, **96**, 2795; (*b*) D. M. P. Mingos, *Inorg. Chem.*, 1973, **12**, 1209; (*c*) J. H. Enemark and R. D. Feltham, *Coord. Chem. Rev.*, 1974, **13**, 339.
36 W. R. Scheidt and J. L. Hoard, *J. Am. Chem. Soc.*, 1973, **95**, 8281.
37 (*a*) H. Nasri, K. J. Haller, Y. Wang, B. H. Huynh and R. Scheidt, *Inorg Chem.*, 1992, **31**, 3459; (*b*) D. S. Bohle and C. H. Hung, *J. Am. Chem. Soc.*, 1995, **117**, 9584.
38 W. R. Scheidt and Y. J. Lee, *Struct. Bonding* (*Berlin*), 1987, **64**, 1.
39 W. Jentzen, M. C. Simpson, J. D. Hobbs, X. Song, T. Ema, N. Y. Nelson, C. J. Medforth, K. M. Smith, M. Veyrat, M. Mazzanti, R. Ramasseul, J.-C. Marchon, T. Takeuchi, W. A. Goddard III and J. A. Shelnutt, *J. Am. Chem. Soc.*, 1995, **117**, 11085.
40 K. M. Kadish, A. Autret, Z. Ou, P. Tagliatesta, T. Boschi and V. Fares, *Inorg. Chem.*, 1997, **36**, 204.
41 D. Mandon, P. Ochsenbein, J. Fisher, R. Weiss, K. Jayaraj, R. N. Austin, A. Gold, P. S. White, O. Brigaud, P. Battioni and D. Mansuy, *Inorg. Chem.*, 1992, **31**, 2044.
42 E. R. Birnbaum, J. A. Hodge, M. W. Grinstaff, W. P. Schaefer, L. Henling, J. A. Labinger, J. E. Bercaw and H. B. Gray, *Inorg. Chem.*, 1995, **34**, 3625.
43 M. W. Grinstaff, M. G. Hill, E. R. Birnbaum, W. P. Schaefer, J. A. Labinger and H. B. Gray, *Inorg. Chem.*, 1995, **34**, 4896.
44 K. M. Kadish, C. Araullo-McAdams, B. C. Han and M. M. Franzen, *J. Am. Chem. Soc.*, 1990, **112**, 8364.
45 M. Madura and W. R. Scheidt, *Inorg. Chem.*, 1976, **15** , 3182.
46 S. G. DiMagno, A. K. Wertsching and C. R. Ross II, *J. Am. Chem. Soc.*, 1995, **117**, 8279.
47 L. D. Sparks, C. J. Medforth, M.-S. Park, J. R. Chamberlain, M. R. Ondrias, M. O. Senge, K. M. Smith and J. A. Shelnutt, *J. Am. Chem. Soc.*, 1993, **115**, 581.
48 W. R. Scheidt, *J. Am. Chem. Soc.*, 1974, **96**, 90.
49 K. M. Kadish, *Prog. Inorg. Chem.*, 1986, **34**, 435.
50 (*a*) F. A. Walker, D. Beroiz and K. M. Kadish, *J. Am. Chem. Soc.*, 1976, **98**, 3484; (*b*) K. M. Kadish, L. A. Bottomley and D. Beroiz, *Inorg. Chem.*, 1978, **17**, 1124.
51 K. M. Kadish, X. H. Mu and X. Q. Lin, *Inorg Chem.*, 1988, **27**, 1489.
52 F. D'Souza, A. Villard, E. Van Caemelbecke, M. Franzen, T. Boschi, P. Tagliatesta and K. M. Kadish, *Inorg. Chem.*, 1993, **32**, 4042.
53 C. K. Johnson, ORTEP, Report ORNL-5138, Oak Ridge National Laboratory, Oak Ridge, TN, 1976.

Paper 8/09719D